A simple protocol for the production of highly deuterated proteins for biophysical studies

Received for publication, March 25, 2022, and in revised form, July 7, 2022 Published, Papers in Press, July 12, 2022,
https://doi.org/10.1016/j.jbc.2022.102253

Jess Li* and **R. Andrew Byrd***

From the Center for Structural Biology, Center for Cancer Research, National Cancer Institute, Frederick, Maryland, USA

Edited by Wolfgang Peti

Highly deuterated protein samples expand the biophysics and biological tool kit by providing, among other qualities, contrast matching in neutron diffraction experiments and reduction of dipolar spin interactions from normally protonated proteins in magnetic resonance studies, impacting both electron paramagnetic resonance and NMR spectroscopy. In NMR applications, deuteration is often combined with other isotopic labeling patterns to expand the range of conventional NMR spectroscopy research in both solution and solid-state conditions. However, preparation of deuterated proteins is challenging. We present here a simple, effective, and user-friendly protocol to produce highly deuterated proteins in *Escherichia coli* cells. The protocol utilizes the common shaker flask growth method and the well-known pET system (which provides expression control *via* the T7 promotor) for large-scale recombinant protein expression. One liter expression typically yields 5 to 50 mg of highly deuterated protein. Our data demonstrate that the optimized procedure produces a comparable quantity of protein in deuterium (^2H_2O) oxide M9 medium compared with that in ^1H_2O M9 medium. The protocol will enable a broader utilization of deuterated proteins in a number of biophysical techniques.

Perdeuteration coupled with isotope labeling has been widely applied and greatly appreciated in the past 2 decades for protein NMR spectroscopy (1–5). Conventional NMR spectroscopy has benefited from uniformly labeled ^{15}N, ^{13}C protein samples, and, when these labeling patterns are combined with replacement of all nonexchangeable protons with deuterons to create a perdeuterated background, it is possible to study very large proteins and protein complexes (6–10). Furthermore, extension of the labeling pattern to include specific methyl group labeling ($^{13}CH_3$), within the context of an otherwise perdeuterated background, enables a still wider range of studies into the structures, binding interactions, and conformational dynamics of proteins and protein complexes (11–13). The combined effect of these sophisticated isotope labelings has permitted researchers tremendous breadth in gaining insights of biological systems and their dynamic interactions, using NMR spectroscopy as the main tool. In recent years, as the biophysical research toolbox expands rapidly, both in terms of technology and instrumentation, it has become very clear that deuteration of proteins and other biomolecular samples will greatly aid in high-quality outcomes for other biophysical applications, particularly small-angle neutron scattering (SANS) (14–17), pulsed double echo electron resonance (DEER) techniques (18–20), and neutron reflectometry (21, 22). The general requirement is to effectively remove, or make nonresponsive, a component of the measurement as a result of perdeuteration, either through contrast matching as in SANS (23) or elongation of relaxation times *via* removal of dipolar coupling as in DEER and NMR (3, 7, 24, 25). The SANS and NMR methods are further enhanced in the context of segmental labeling (26–29), wherein portions of a macromolecule may be prepared with deuteration for SANS (and/or isotopic labeling for NMR) and the other portions are protonated. Hence, the need for an efficient, reproducible protocol for high-level deuteration is broadly applicable to numerous experimental methods.

Although highly desired, deuterated (^2H) sample preparation has been notoriously problematic. Most researchers find it arduous and inconsistent. Bacterial cells (*Escherichia coli*) are the preferred host, as insect and mammalian cells are difficult to culture in a D_2O medium (30–32). Even bacteria can be difficult to adapt to grow in high levels of D_2O (33). Conventional procedures are time consuming and labor intensive, and the yield of deuterated samples, where the percentage labeling is >90%, can be very low. In our laboratory, we previously examined two commonly used methods: (1) medium switch prior to induction and (2) multistep media switch adaptation. In method (1), cells were grown in LB medium to the appropriate density for induction ($A_{600} \sim 0.8$), pelleted by centrifugation, resuspended in 100% D_2O medium, and induced immediately. This method often leads to complete cell death during induction, due to lack of proper adaptation. If cells do survive, the level of protein expression is very low. In method (2), the multistep media switch adaptation, cells were grown and transferred, stepwise, from LB to 50%, 75%, and 100% D_2O media, which discards considerable isotopic media in the adaptation phase. This method also results in low protein expression due to multiple centrifugation and resuspension steps, rendering a generally unhealthy cell culture. The approximate yield of deuterated proteins from these methods is less than 25% of the yield from our current protocol reported here. When expression efficiency is low, the combined cost of D_2O,

* For correspondence: R. Andrew Byrd, byrdra@mail.nih.gov; Jess Li, lije@mail.nih.gov.

$^{15}N/^{13}C$ sources, and/or specific ^{13}C-labeled metabolic precursor compounds can become very high, thus limiting widespread application and realization of the full potential.

We report a highly reproducible, user friendly, time and isotope efficient, and high percentage labeling deuteration procedure that can support the ever-expanding applications in the extended communities. Our protocol eliminates many of the common roadblocks: (1) the carryover of any rich medium (LB, Superbroth, etc.) into the final culture; (2) multiple media transfers during cell training, which involves repetitive cell pelleting, resulting in long recovery time for bacterial cells and unhealthy growth; (3) extended growth period that requires lengthy in-person monitoring; (4) an unhealthy cell growth curve that often leads to low expression and even cell death.

Results

The key to successful cell growth in deuterated medium (^{2}H-M9; for abbreviations and media descriptions see Experimental procedures) is maintaining cell density in the exponential phase (Fig. 1*A*). The protocol keeps A_{600} at or slightly above 0.2 each time a culture is initiated or transferred or following a dilution. This approach ensures that the cells are the most healthy and viable to adapt into a higher D_2O percentage environment. The protocol is described for production of 1 liter ^{2}H-M9 expression medium. LB and ^{1}H-M9 cultures do not require training (adaptation). A modified simple protocol for expression in LB and ^{1}H-M9 is described in the Supporting information and illustrated in Figure 1*B*.

A schematic flow chart for expression of deuterated proteins in ^{2}H-M9 is illustrated in Figure 2. In general, the flask (tube) used for cell growth is 4 to 10 times the volume of the culture, which ensures proper aeration during growth. Cultures are shaken in a temperature-regulated incubator at 250 rpm. Antibiotics are chosen based on the vectors in which the genes are constructed and added to all media for a given protein expression. Carbenicillin is preferred over ampicillin for stability, and all media should be stored at 4 °C.

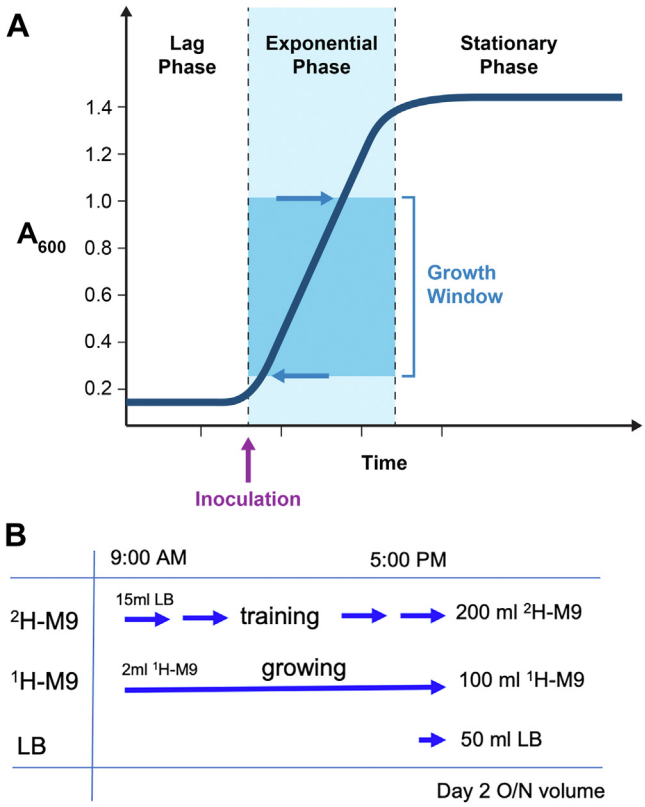

Figure 1. Nominal growth curve and comparative day 2 growths on different media. *A*, nominal bacterial growth curve. Growth is monitored by the A_{600}, rather than the typical doubling time. A_{600} from 0.2 to 1.0 is the preferred growth window. Cell density at initial inoculation and each expanding step is maintained at ~0.2 to 0.3 for healthy growth, time-saving, and fast amplification. *B*, a general timeline for day 2 cell culture in all three media. ^{2}H-M9 culture goes through training as described in Figure 2. For ^{1}H-M9, a small 2 ml starter culture is grown during the day to reach A_{600} ~0.2 to 0.3, then added into 100 ml media for overnight growth. For LB growth, inoculate a dozen colonies directly into 50 ml media for overnight. Note, day 2 overnight culture volumes are different for each media reflecting the cell density in each media after overnight growth, with LB at the highest, ^{2}H-M9 at the lowest. By adjusting the volume accordingly, the initial cell density on day 3 is ensured to be around 0.2, thus maintaining the exponential growth window.

Protocol

Day 1

1. Perform fresh transformation of plasmid DNA into BL21* competent cells.
2. Plate on LB agar with proper antibiotic selection.
3. Grow overnight at 37 °C.
4. Aim to produce a plate with fresh, well-isolated colonies. Frozen cell stocks are not preferred for $^{2}H_2O$ medium growth.
5. Prepare 1 liter of the desired labeling medium, *e.g.*, ^{1}H-M9(^{15}N) or ^{2}H-M9(^{15}N); store at 4 °C.

Day 2

1. Inoculate 15 ml LB media (in a 250-ml flask) with about two dozen freshly transformed colonies. The general guideline is to use enough colonies so that A_{600} can reach ~0.4 to 0.5 after about 2-h growth at 37 °C.
2. Allow the initial 15 ml LB to grow to A_{600} ~0.4 to 0.5, add 15 ml of ^{2}H-M9 medium in the same flask to a total volume of 30 ml, which is now ~50% in $^{2}H_2O$. Continue growth at 37 °C.
3. When the 30 ml culture (~50% in $^{2}H_2O$) reaches A_{600} ~0.4 to 0.5 (usually in approximately 1 h), add 30 ml of ^{2}H-M9 medium to a total volume of 60 ml (in the same 250-ml flask, now at 75% $^{2}H_2O$). Continue growth at 37 °C until A_{600} ~0.4 to 0.5 (in approximately 1 h).
4. Centrifuge the cells (10 min, 3000*g*), discard the medium, and resuspend the cell pellet in 100 ml fresh ^{2}H-M9 medium (in a 500-ml flask, now at 100% $^{2}H_2O$).
5. Continue to grow at 37 °C for approximately 1 h to allow the cells to acclimate to the 100% $^{2}H_2O$ environment. Finally, add 100 ml ^{2}H M9 medium, reaching a total culture of 200 ml. Let growth continue at 37 °C overnight.

Day 3

1. Record the A_{600} following overnight growth, which should be approximately 1.3 to 1.5.

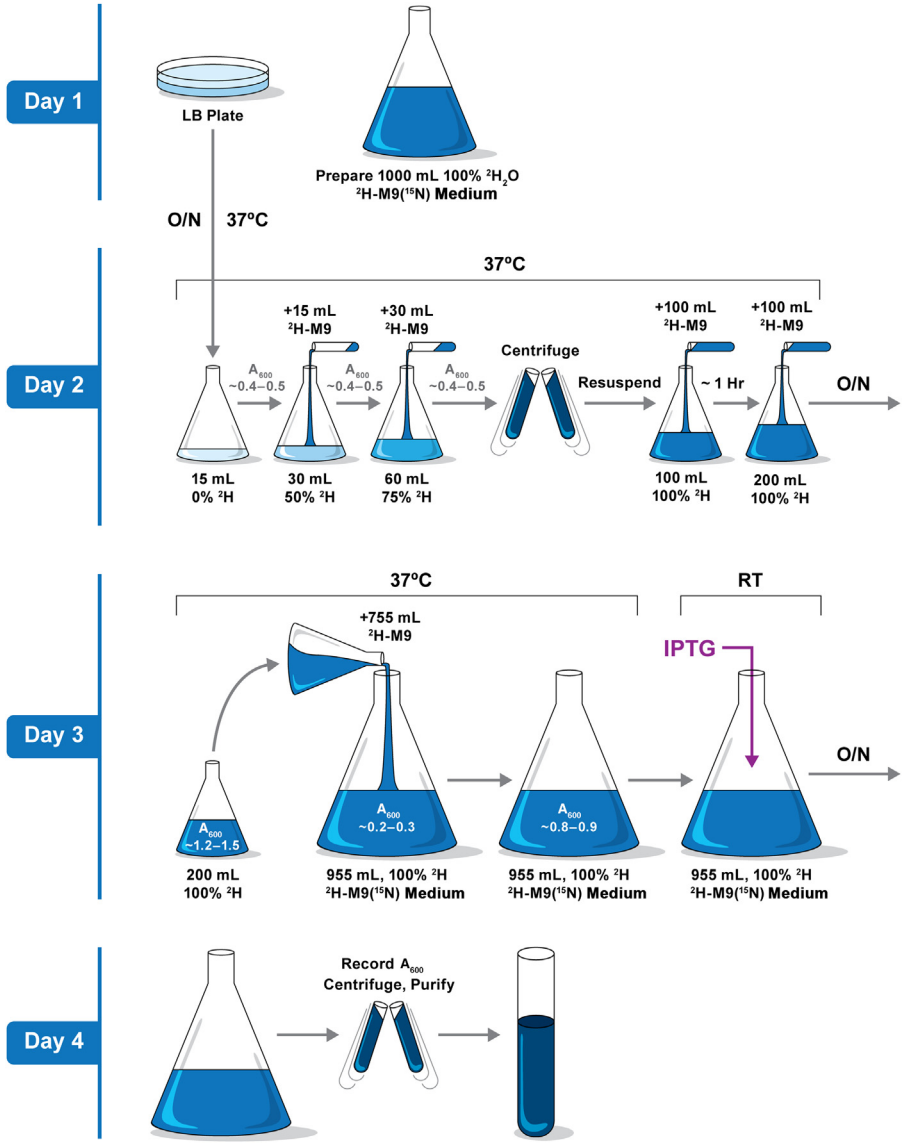

Figure 2. Schematic illustration of 1 liter ^{2}H-M9 expression including cell adaptation. Variations to induction conditions are described in the text for individual protein expression.

2. Combine the 200 ml culture with the remaining 755 ml of ^{2}H-M9 medium in a 4-l flask, and record the A_{600}, which should be ~0.2 to 0.3.
3. Continue to grow at 37 °C and monitor A_{600}. Cells usually double in density every 2 h in ^{2}H-M9; allow cells to double twice to about A_{600} = 0.8 to 0.9.
4. If needed, supply additives specific to the desired sample, such as precursors for custom isotope labels or prosthetic groups for posttranslational modifications or other supplementary elements.
   - For methyl labeling, appropriate metabolic precursors (*e.g.*, α-keto acids (5, 12, 34)) should be added according to manufacturer instructions. For example, to label stereospecific ^{13}C-Ile, -Leu, and -Val, the appropriate kit (TLAM-I$^{\sigma 1}$-LV^{proS}, NMR-Bio) was added to the medium 30 min prior to IPTG induction. For myr-Arf1, addition of 50 mg sodium myristate and 50 mg coenzyme A are needed for posttranslational myristoylation. Other supplementary elements, such as Zn^{2+}, which is required for high expression of ASAP1 PZA, can also be added at this growth stage, 30 min prior to IPTG induction.
5. Induce protein expression, wherein the temperature and duration time will vary based on the nature of proteins to be overexpressed.
   - Generally, cultures are cooled down (while shaking) for approximately 30 min in a shaker adjusted to room temperature. Cell density will expand moderately to about 0.9 to 1.0 A_{600} during cool down. Induction is initiated by adding IPTG to 0.2 mM, and growth is continued at room temperature overnight. These cells are harvested in the morning of day 4. Specifically in this comparative study, the general procedure is followed for ASAP1 PH, ASAP1 PZA, and myr-Arf1; however, for Ube2g2, gp78c, and MSPDH5, cultures are maintained at

37 °C for 30 min after supplying additives and then induced with 1 mM IPTG for 3 h. Cells are harvested at the end of day 3. This 37 °C induction modification is necessary based on our knowledge and extensive testing on these proteins. We find that a significant number of mammalian proteins overexpressed in *E. coli* cells exhibit some level of toxicity, which can lead to reduced or completely abolished expression when induced at room temperature overnight. We recommend researchers test both induction conditions for their proteins of interest.

Day 4

1. Record A_{600} of the final culture and collect a 20-μl sample for SDS-PAGE analysis.
2. Harvest cells by centrifugation (10 min, 3000*g*) and either proceed with protein-specific purification or store the cell pellet at −80 °C.

As demonstration of the generality of this protocol, we provide data for the expression of six different mammalian proteins. The proteins span a wide range of protein types and sizes, comprising a moderate-size single-domain ubiquitin-conjugating E2 enzyme (Ube2g2) (24, 35, 36), an isolated domain of a more complex multidomain protein (PH domain of ASAP1) (21), a multidomain signaling protein (PZA of ASAP1) (37), a posttranslationally modified (*via* myristoylation) protein (myr-Arf1) (38), a complex multidomain protein with internal intrinsically disordered regions (gp78C) (35, 36, 39), and the amphipathic membrane scaffolding protein (MSPΔH5) used to build nanodisc membrane mimetic particles (40, 41). Each of these systems have been expressed with high levels of deuteration (≥96%), combined with either ^{15}N or complex $^{13}CH_3$-methyl labels. These proteins vary in size, expression level, solubility, etc., proving the flexibility and efficiency of the protocol.

The comparative performance for the six proteins is demonstrated by parallel expression in three different media: (1) LB, (2) ^{1}H-M9(^{15}N), (3) ^{2}H-M9(^{15}N) (Fig. 3). It is observed that expression levels, when following this protocol, are nearly equivalent for ^{1}H-M9(^{15}N) and ^{2}H-M9(^{15}N), and expression is only moderately reduced from LB. Each protein was purified according to the published procedures, and mass spectral data were acquired to enable determination of labeling efficiency (Table 1). In each case, the ^{15}N-labeling efficiency corresponds closely to the 99% ^{15}N enrichment of the nitrogen source, $^{15}NH_4Cl$. Furthermore, the labeling efficiency of ^{2}H, in the nonexchangeable positions, exceeds 96% for all six proteins. Each of these proteins can be prepared and purified in 5- to 50-mg/l quantities (data not shown), thus supporting a wide variety of structural and biophysical studies. In addition, we have observed that the expression level and the percentage of deuteration are not affected by other supplementary additives (such as a-keto acid precursors) in the medium, provided the carbon source ($^{12}C_6{}^{2}H_7$-glucose or $^{13}C_6{}^{2}H_7$-glucose) is ≥97% deuterated (data not shown).

Discussion

The described procedure (Fig. 2) has been employed in our laboratory for the past decade. We confidently report that we can express the 30+ proteins from a wide range of difficult systems in highly deuterated form at similar or slightly reduced level compared with the expression in rich medium such as LB or protonated ^{1}H-M9 (^{15}N) medium. One of the keys to this protocol is proper attention to cell viability and avoidance of cellular and metabolic stress. Our approach deviates from conventional adaptation methods that encompass multiple steps of cell pelleting, media transfer, and resuspension. All these treatments incur additional stress and slow down, or endanger, cell growth. Unlike other published methods (42), this protocol is significantly simplified, wherein only two types of culture media (15 ml LB and 1 liter ^{2}H-M9) are needed for each 1 liter production. We achieve such simplicity by starting a small, healthy LB culture and expanding (by simple dilution) the LB culture with ^{2}H-M9 medium in a stepwise fashion, while maintaining the growth within the exponential phase through all media adjustments. Another advantage of the protocol is that there is no carryover of any initial LB/H_2O media into the final expression culture, since we complete adaptation to 100% D2O at the end of day 2, which leads to the high percentage of deuteration (Table 1). In addition, the protocol is time efficient, as the total time from initial cell culture in day 2 to the harvest on the morning of day 4 is approximately 48 h. The effective use of time is achieved by two elements: (1) starting with a fresh, healthy culture in LB (H_2O) medium and (2) adapting cells to a higher D_2O medium by stepwise addition of ^{2}H-M9 medium, thus eliminating multiple cell-pelleting steps.

Another protein deuteration method (43, 44) has encouraged high cell density growth combined with reduced culture volume. While this approach may be desirable for reducing the cost of isotope labels and D_2O, the high cell density growth (A_{600} = 6.0–10.0) may incur unforeseeable cellular and metabolic stress and may not be commonly applicable for a wide range of proteins. Our protocol emphasizes healthy cell growth and is mindful of minimizing the waste of D_2O. Overall, only 45 ml of ^{2}H-M9 medium is discarded during cell adaptation per liter of growth production.

Interestingly, by observing the induced protein band intensity (Fig. 3), we find that, on average, most proteins express at a similar level across the three media. The minor changes presumably result from the characteristics of each protein. Contrary to conventional wisdom, not all proteins show reduced expression in M9 medium. Although some do show reduced expression, such as ASAP1-PH, ASAP-PZA, and myr-Arf1, others such as Ube2g2, gp78c, and MSPΔH5 express slightly better in M9 medium than in LB. One possible explanation is cell toxicity caused by low-level, basal expression in rich media (often called “leaky vectors”), while in M9 medium, basal expression is largely suppressed.

These flexible, combined labeling strategies further expand both NMR (21, 26) and SANS applications (16, 45). For NMR applications, in addition to performing ^{15}N-labeling in the presence of deuteration, we can perform the full variety of

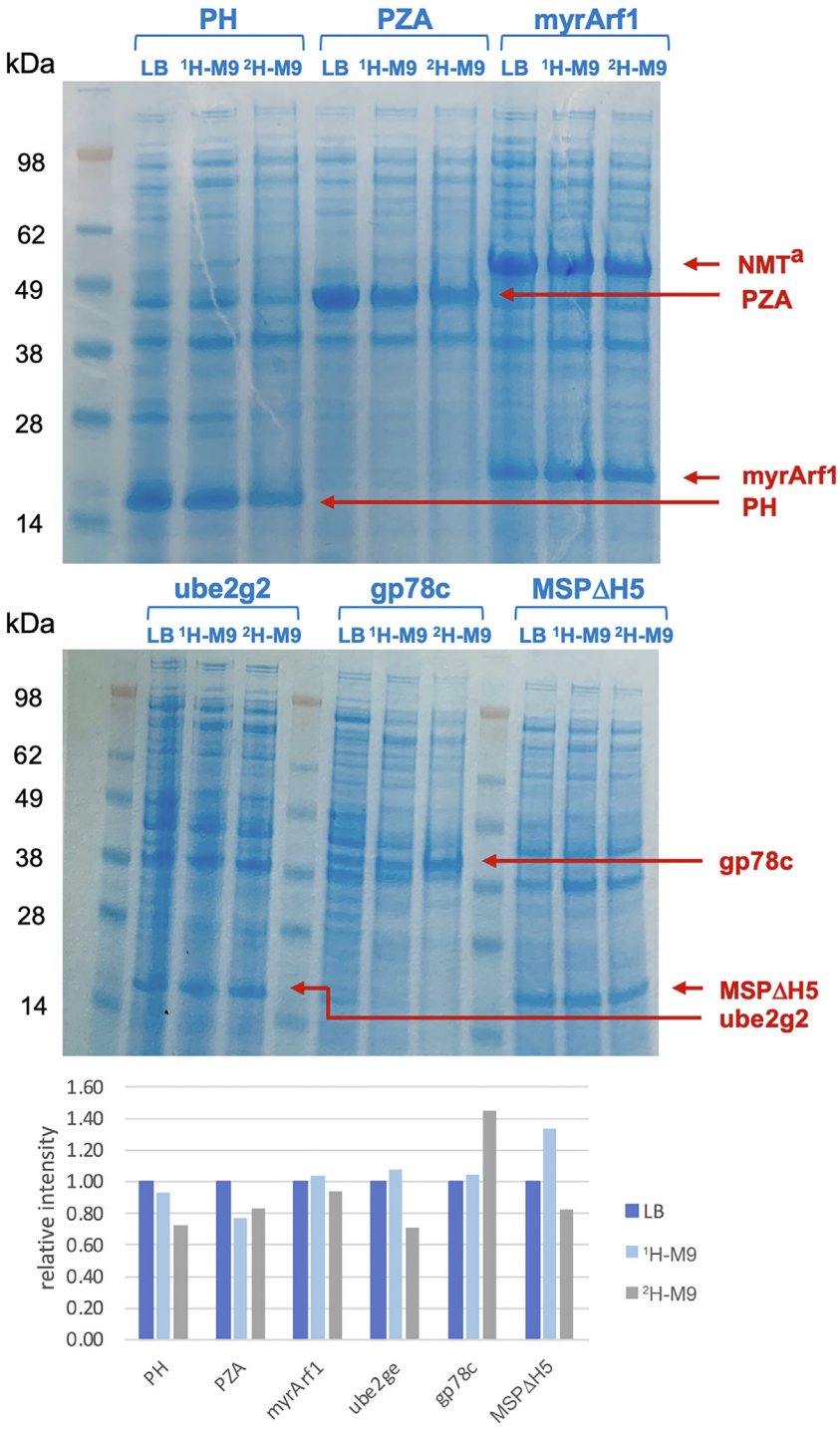

Figure 3. Comparative expression of six different proteins. Each protein is expressed in parallel using three types of media: LB, ^{1}H-M9, and ^{2}H-M9. IPTG-induced products are marked with *red arrows*. Samples are collected before harvest centrifugation. A 20-µl aliquot of each culture is mixed with 20 µl 2xSDS sample buffer, denatured at 95 °C for 30 min. Equal amounts of sample (20 µl) are loaded in each lane on SDS-PAGE gel. Relative intensities from digitization of bands for LB, ^{1}H-M9, and ^{2}H M-9 are shown for all six proteins, respectively. [a]NMT (N-myristoyltransferase) is coexpressed with Arf1 for posttranslational modification.

methyl-specific labeling (12, 34, 46) that has become popular in NMR studies. These labeling schemes include stereospecific, uniform side-chain labeling or suppression of specific residue types. For example, the ^{1}H-^{13}C methyl transverse relaxation optimized spectroscopy (Fig. S1*A*) and the ^{1}H-^{15}N transverse relaxation optimized spectroscopy (Fig. S1*B*) spectra of ^{2}H, ^{15}N, ILV^{proS} ^{13}CH$_3$-labeled ASAP1 PZA illustrate the high spectral quality, sensitivity, and resolution that are afforded by the labeling scheme when precursors for methyl labeling are included. ASAP1 PZA is a 44.5-kDa multidomain protein that binds to membrane-associated Arf1 (21, 37, 38), and NMR studies of these interactions at a nanodisc membrane surface require high levels of deuteration, as a protonated sample would result in highly overlapping, very broad, and weak

Table 1
Mass spectrometry data and isotopic labeling efficiencies

Protein	No. residues	Mass value	Unlabeled mass (Da)	^{15}N-labeled mass (Da)	%^{15}N-labeled	^{15}N/^{2}H-labeled mass[a] (Da)	% ^{2}H-labeled in^{15}N/^{2}H[a]
ASAP1-PH	131	Predicted[b]	15107.4	15307.8		16087.5	
		Measured	15,107	15,306	99.3	16,074	98.5
myr-Arf1	190	Predicted[b]	21885.8	22158.3		23306.0	
		Measured	21,884	22,154	99.1	23,294	99.3
Ube2g2	164	Predicted[b]	18459.6	18665.9		19671.9	
		Measured	18,459	18,665	99.6	19,625	96.4
gp78c	309	Predicted[b]	32532.3	32950.8		34507.1	
		Measured	32,533	32,945	98.4	34,487	99.1
MSPl'.H5	183	Predicted[b]	21336.1	21603.6		22724.3	
		Measured	21,333	21,599	99.4	22,706	98.8
ASAP1-PZA	400	Predicted[b]	44564.1	45104.0		47482.3	
		Measured	44,563	45,093	98.2	47,429	98.2

[a] Mass represents the replacement of nonexchangeable protons with ^{2}H. All exchangeable -NH, -NH$_2$, -SH, -OH, and -COOH protons are calculated as ^{1}H, representing back exchange during purification and mass spectrometry analyses. The mass spectrometry analyses were performed on an electrospray LC-MS that ensures full protonation of all exchangeable sites. The calculations were performed with the software package Protein Sequence Analysis, developed by Ira Palmer, NIH.
[b] Predicted mass computed using the amino acid sequence and the software package Protein Sequence Analysis, developed by Ira Palmer, NIH.

signals. The protocol and labeling scheme have also been combined with segmental labeling (26), wherein only one domain of the multidomain PZA is deuterated or ^{15}N and ^{13}C labeled. We have utilized highly deuterated proteins to minimize background relaxation and enable more accurate measurement of long-range, intermolecular paramagnetic relaxation effects (Zhang *et al.*, in preparation and (21)), facilitate solid-state ^{1}H-detected NMR (2, 47), and DEER experiments utilizing nanodisc particles (Fig. S2, and (19)). For SANS applications, it can be advantageous to adjust the percentage of deuteration to provide optimal contrast matching in multicomponent systems (23), including protein:protein complexes (16) and membrane systems (14, 15). Since our protocol provides for complete control of ^{2}H-labeling for nonexchangeable hydrogen atoms, it will be possible to fine-tune the level of deuteration. Adjustment of the final $^{2}H_2O$ concentration and the ratio of $^{1}H_7$-glucose to $^{2}H_7$-glucose in the medium can achieve a specific level of deuteration, which can be readily monitored by mass spectrometry of the expressed protein.

The protocol has proven general and enables the use of deuteration to enhance NMR and other biophysical methodologies. The protocol should facilitate and expand the application of perdeuteration in a range of biophysical experiments and enable a broad range of systems to be examined in exquisite detail. Such studies will lead to better functional understanding and mechanistic detail in many biological systems.

Experimental procedures

Protein expression

Each of the six proteins were expressed in *E. coli* BL21 star (DE3) cells according to the protocol presented in Figure 2. Any adjustment of conditions followed published procedures for the individual protein, as noted in Results.

Mass spectrometry

Mass spectrometry data were acquired on an Agilent 6130 Quadrupole LC/MS System (Agilent Technologies, Inc) equipped with an electrospray source, operated in positive-ion mode. Separation was performed on a 300SB-C3 Poroshell column (2.1 mm × 75 mm; particle size 5 μm). The analytes were eluted at a flow rate of 1 ml/min with a 5 to 100% organic gradient over 5 min and holding the organic phase A for 1 min. Mobile phase A contained 5% acetic acid in water and mobile phase B was acetonitrile. Data acquisition, data analysis, and deconvolution of mass spectra were performed using Open Lab Chem Station Edition software (version C.01.05). Samples of purified proteins were typically 5 μl of a 5 μM solution.

Materials

Isotopically labeled compounds were obtained commercially from the following sources:

Cambridge Isotope Laboratories: deuterium oxide ($^{2}H_2O$, Product no. DLM-4), a-keto acids (product no. CDLM-7317, CDLM-7318, etc.).

Millipore Sigma/Isotech: ^{15}N-ammonium chloride (product no. 299251), $^{13}C_6{}^{2}H_7$-glucose (product no. 552151), $^{12}C_6{}^{2}H_7$-glucose (product no. 552003).

NMR-Bio: TLAM-I$^{\delta 1}$LVpro^{S}, TLAM- I$^{\delta 1}$MT, and other specialty labeling kits; for residue type and stereospecific $^{13}CH_3$-labeling, see http://www.nmr-bio.com.

Solutions and abbreviations

1. M9: minimal medium described by Neidhart *et al.* (48), where the nitrogen source is derived from NH_4Cl and the carbon source is derived from glucose. Both the nitrogen and carbon source can be supplied with ^{15}N or ^{13}C. In addition, the carbon source can be supplied as $^{12}C_6{}^{1}H_7$-glucose, $^{13}C_6{}^{1}H_7$-glucose, $^{12}C_6{}^{2}H_7$-glucose, or $^{13}C_6{}^{2}H_7$-glucose (the full recipe is provided in the Supporting information).
2. ^{1}H-M9: M9 minimal medium wherein the solvent is $^{1}H_2O$.
3. ^{2}H-M9: M9 minimal medium wherein the solvent is $^{2}H_2O$ (99.9% ^{2}H), the nitrogen source is natural abundance $^{14}NH_4Cl$, and the carbon source is natural abundance $^{12}C_6{}^{2}H_7$ glucose (97% ^{2}H).
4. ^{1}H-M9(^{15}N): M9 minimal medium wherein the solvent is $^{1}H_2O$, the nitrogen source is $^{15}NH_4Cl$ (>98% ^{15}N), and the carbon source is natural abundance $^{12}C_6{}^{1}H_7$-glucose.

5. ^{2}H-M9(^{15}N): M9 minimal medium wherein the solvent is $^{2}H_2O$ (99.9% ^{2}H), the nitrogen source is $^{15}NH_4Cl$ (>98% ^{15}N), and the carbon source is natural abundance ^{12}C and ^{2}H-labeled $^{12}C_6{}^{2}H_7$-glucose (97% ^{2}H).
6. ^{2}H-M9(^{15}N, ^{13}C): M9 minimal medium wherein the solvent is $^{2}H_2O$ (99.9% ^{2}H), the nitrogen source is $^{15}NH_4Cl$ (>98% ^{15}N), and the carbon source is $^{13}C_6{}^{2}H_7$-glucose (99% ^{13}C and 97% ^{2}H).
7. ^{2}H-M9(^{15}N, ^{13}C-methyl): M9 minimal medium wherein the solvent is $^{2}H_2O$ (≥99% ^{2}H), the nitrogen source is $^{15}NH_4Cl$ (>98% ^{15}N), the general carbon source is $^{12}C_6{}^{2}H_7$-glucose (97% ^{2}H), and specific metabolic precursors to label the methyl groups of Met, Ala, Val, Leu, Ile, and/or Thr are provided (34).
8. LB: *Luria Broth* medium made according to manufacturer's prescription in $^{1}H_2O$ solvent. MP Biomedicals, cat. No. 3002136, formulated as 4 capsules/l in double distilled H_2O and autoclaved.
9. LB/carb or LB/Kan: *Luria Broth* medium made according to manufacturer's prescription in $^{1}H_2O$ solvent containing 100 mg/l of carbenicillin or 50 mg/l of kanamycin.
10. LB plate: Agar plate made with LB/carb or LB/kan medium.
11. IPTG: isopropyl β-D-1-thiogalactopyranoside.

Data availability

All data are contained within the article. Copies of the datasets used and/or analyzed during the current study are available from the corresponding author on reasonable request. The software, Protein Sequence Analysis, is available from Ira Palmer, NIAMS, NIH (palmeri@mail.nih.gov), and numerous other online variants exist for computing mass from primary sequence.

Supporting information—This article contains supporting information (48–50).

Acknowledgements—We are grateful to the cadre of postdoctoral fellows and postbaccalaureate fellows who have worked on different projects through the years to apply this methodology. Particularly, we would like to thank Ranabir Das, Yifei Li, Olivier Soubias, Domarin Khago, Yue Zhang, Fa-An Chao, Ian Fucci, Brianna Papoutsis, Kristen Snitchler, and Cameron McGlone. We thank Yue Zhang for the sample preparation and NMR spectra reported in Fig. S1, and we are grateful for the DEER spectra (Fig. S2) acquired by Dr James Baber, NIDDK, National Institutes of Health. We acknowledge the use of the Biophysics Resource, Center for Structural Biology, NCI, National Institutes of Health and the assistance of S. Tarasov and M. Dyba. The research is supported by the Intramural Research Program of the National Cancer Institute, National Institutes of Health Projects ZIA BC 011419, ZIA BC 011131, and ZIA BC 011132. The content is solely the responsibility of the authors and does not necessarily represent the official views of the National Institutes of Health.

Author contributions—J. L. and R. A. B. conceptualization; J. L. methodology; J. L. investigation; R. A. B. resources; R. A. B. writing-original draft; J. L. and R. A. B. writing – review and editing; R. A. B. supervision; R. A. B. project administration; R. A. B. funding acquisition.

Conflict of interest—The authors declare that they have no conflicts of interest with the contents of this article.

Abbreviations—The abbreviations used are: DEER, double echo electron resonance; SANS, small-angle neutron scattering.

References

1. Walters, K. J., Matsuo, H., and Wagner, G. (1997) A simple method to distinguish intermonomer nuclear overhauser effects in homodimeric proteins with C-2 symmetry. *J. Am. Chem. Soc.* **119**, 5958–5959
2. Morcombe, C. R., Gaponenko, V., Byrd, R. A., and Zilm, K. W. (2004) Diluting abundant spins by isotope edited radio frequency field assisted diffusion. *J. Am. Chem. Soc.* **126**, 7196–7197
3. Reif, B. (2022) Deuteration for high-resolution detection of protons in protein magic angle spinning (MAS) solid-state NMR. *Chem. Rev.* **122**, 10019–10035
4. Gardner, K. H., Rosen, M. K., and Kay, L. E. (1997) Global folds of highly deuterated, methyl-protonated proteins by multidimensional NMR. *Biochemistry* **36**, 1389–1401
5. Tugarinov, V., Kanelis, V., and Kay, L. E. (2006) Isotope labeling strategies for the study of high-molecular-weight proteins by solution NMR spectroscopy. *Nat. Protoc.* **1**, 749–754
6. Pervushin, K., Riek, R., Wider, G., and Wuthrich, K. (1997) Attenuated T2 relaxation by mutual cancellation of dipole-dipole coupling and chemical shift anisotropy indicates an avenue to NMR structures of very large biological macromolecules in solution. *Proc. Natl. Acad. Sci. U. S. A.* **94**, 12366–12371
7. Tugarinov, V., Hwang, P. M., and Kay, L. E. (2004) Nuclear magnetic resonance spectroscopy of high-molecular-weight proteins. *Annu. Rev. Biochem.* **73**, 107–146
8. Rosenzweig, R., and Kay, L. E. (2014) Bringing dynamic molecular machines into focus by methyl-TROSY NMR. *Annu. Rev. Biochem.* **83**, 291–315
9. Fiaux, J., Bertelsen, E. B., Horwich, A. L., and Wuthrich, K. (2004) Uniform and residue-specific 15N-labeling of proteins on a highly deuterated background. *J. Biomol. NMR* **29**, 289–297
10. Sattler, M., and Fesik, S. W. (1996) Use of deuterium labeling in NMR: overcoming a sizeable problem. *Structure* **4**, 1245–1249
11. Alderson, T. R., and Kay, L. E. (2021) NMR spectroscopy captures the essential role of dynamics in regulating biomolecular function. *Cell* **184**, 577–595
12. Rossi, P., Monneau, Y. R., Xia, Y., Ishida, Y., and Kalodimos, C. G. (2019) Toolkit for NMR studies of methyl-labeled proteins. *Methods Enzymol.* **614**, 107–142
13. Chao, F. A., Dharmaiah, S., Taylor, T., Messing, S., Gillette, W., Esposito, D., *et al.* (2022) Insights into the cross talk between effector and allosteric lobes of KRAS from methyl conformational dynamics. *J. Am. Chem. Soc.* **144**, 4196–4205
14. Maric, S., Skar-Gislinge, N., Midtgaard, S., Thygesen, M. B., Schiller, J., Frielinghaus, H., *et al.* (2014) Stealth carriers for low-resolution structure determination of membrane proteins in solution. *Acta Crystallogr. D Biol. Crystallogr.* **70**, 317–328
15. Bengtsen, T., Holm, V. L., Kjolbye, L. R., Midtgaard, S. R., Johansen, N. T., Tesei, G., *et al.* (2020) Structure and dynamics of a nanodisc by integrating NMR, SAXS and SANS experiments with molecular dynamics simulations. *Elife* **9**, e56518
16. Wilamowski, M., Hammel, M., Leite, W., Zhang, Q., Kim, Y., Weiss, K. L., *et al.* (2021) Transient and stabilized complexes of Nsp7, Nsp8, and Nsp12 in SARS-CoV-2 replication. *Biophys. J.* **120**, 3152–3165
17. Neylon, C. (2008) Small angle neutron and X-ray scattering in structural biology: recent examples from the literature. *Eur. Biophys. J.* **37**, 531–541
18. Schmidt, T., Walti, M. A., Baber, J. L., Hustedt, E. J., and Clore, G. M. (2016) Long distance measurements up to 160 A in the GroEL

tetradecamer using Q-band DEER EPR spectroscopy. *Angew. Chem. Int. Ed. Engl.* **55**, 15905–15909
19. Bibow, S., Polyhach, Y., Eichmann, C., Chi, C. N., Kowal, J., Albiez, S., *et al.* (2017) Solution structure of discoidal high-density lipoprotein particles with a shortened apolipoprotein A-I. *Nat. Struct. Mol. Biol.* **24**, 187–193
20. Jeschke, G. (2012) DEER distance measurements on proteins. *Annu. Rev. Phys. Chem.* **63**, 419–446
21. Soubias, O., Pant, S., Heinrich, F., Zhang, Y., Roy, N. S., Li, J., *et al.* (2020) Membrane surface recognition by the ASAP1 PH domain and consequences for interactions with the small GTPase Arf1. *Sci. Adv.* **6**, eabd1882
22. Clifton, L. A. (2021) Unravelling the structural complexity of protein-lipid interactions with neutron reflectometry. *Biochem. Soc. Trans.* **49**, 1537–1546
23. Heller, W. T. (2010) Small-angle neutron scattering and contrast variation: a powerful combination for studying biological structures. *Acta Crystallogr. D Biol. Crystallogr.* **66**, 1213–1217
24. Chakrabarti, K. S., Li, J., Das, R., and Byrd, R. A. (2017) Conformational dynamics and allostery in E2:E3 interactions drive ubiquitination: gp78 and Ube2g2. *Structure* **25**, 794–805.e5
25. Chao, F. A., Li, Y., Zhang, Y., and Byrd, R. A. (2019) Probing the broad time scale and heterogeneous conformational dynamics in the catalytic core of the Arf-GAP ASAP1 via methyl adiabatic relaxation dispersion. *J. Am. Chem. Soc.* **141**, 11881–11891
26. Li, J., Zhang, Y., Soubias, O., Khago, D., Chao, F. A., Li, Y., *et al.* (2020) Optimization of sortase A ligation for flexible engineering of complex protein systems. *J. Biol. Chem.* **295**, 2664–2675
27. LaPorte, S. L., Juo, Z. S., Vaclavikova, J., Colf, L. A., Qi, X., Heller, N. M., *et al.* (2008) Molecular and structural basis of cytokine receptor pleiotropy in the interleukin-4/13 system. *Cell* **132**, 259–272
28. Freiburger, L., Sonntag, M., Hennig, J., Li, J., Zou, P., and Sattler, M. (2015) Efficient segmental isotope labeling of multi-domain proteins using Sortase A. *J. Biomol. NMR* **63**, 1–8
29. Michel, E., and Allain, F. H. (2015) Selective amino acid segmental labeling of multi-domain proteins. *Methods Enzymol.* **565**, 389–422
30. Franke, B., Opitz, C., Isogai, S., Grahl, A., Delgado, L., Gossert, A. D., *et al.* (2018) Production of isotope-labeled proteins in insect cells for NMR. *J. Biomol. NMR* **71**, 173–184
31. Kofuku, Y., Ueda, T., Okude, J., Shiraishi, Y., Kondo, K., Mizumura, T., *et al.* (2014) Functional dynamics of deuterated beta2 -adrenergic receptor in lipid bilayers revealed by NMR spectroscopy. *Angew. Chem. Int. Ed. Engl.* **53**, 13376–13379
32. Clark, L., Zahm, J. A., Ali, R., Kukula, M., Bian, L., Patrie, S. M., *et al.* (2015) Methyl labeling and TROSY NMR spectroscopy of proteins expressed in the eukaryote Pichia pastoris. *J. Biomol. NMR* **62**, 239–245
33. O'Brien, E. S., Lin, D. W., Fuglestad, B., Stetz, M. A., Gosse, T., Tommos, C., *et al.* (2018) Improving yields of deuterated, methyl labeled protein by growing in H2O. *J. Biomol. NMR* **71**, 263–273
34. Gans, P., Hamelin, O., Sounier, R., Ayala, I., Dura, M. A., Amero, C. D., *et al.* (2010) Stereospecific isotopic labeling of methyl groups for NMR spectroscopic studies of high-molecular-weight proteins. *Angew. Chem. Int. Ed. Engl.* **49**, 1958–1962
35. Das, R., Mariano, J., Tsai, Y. C., Kalathur, R. C., Kostova, Z., Li, J., *et al.* (2009) Allosteric activation of E2-RING finger-mediated ubiquitylation by a structurally defined specific E2-binding region of gp78. *Mol. Cell* **34**, 674–685
36. Das, R., Liang, Y. H., Mariano, J., Li, J., Huang, T., King, A., *et al.* (2013) Allosteric regulation of E2:E3 interactions promote a processive ubiquitination machine. *EMBO J.* **32**, 2504–2516
37. Che, M. M., Boja, E. S., Yoon, H. Y., Gruschus, J., Jaffe, H., Stauffer, S., *et al.* (2005) Regulation of ASAP1 by phospholipids is dependent on the interface between the PH and Arf GAP domains. *Cell Signal.* **17**, 1276–1288
38. Li, Y., Soubias, O., Li, J., Sun, S., Randazzo, P. A., and Byrd, R. A. (2019) Functional expression and characterization of human Myristoylated-Arf1 in nanodisc membrane mimetics. *Biochemistry* **58**, 1423–1431
39. Liu, S., Chen, Y., Li, J., Huang, T., Tarasov, S., King, A., *et al.* (2012) Promiscuous interactions of gp78 E3 ligase CUE domain with polyubiquitin chains. *Structure* **20**, 2138–2150
40. Hagn, F., Etzkorn, M., Raschle, T., and Wagner, G. (2013) Optimized phospholipid bilayer nanodiscs facilitate high-resolution structure determination of membrane proteins. *J. Am. Chem. Soc.* **135**, 1919–1925
41. Denisov, I. G., and Sligar, S. G. (2017) Nanodiscs in membrane biochemistry and biophysics. *Chem. Rev.* **117**, 4669–4713
42. Cai, M., Huang, Y., Yang, R., Craigie, R., and Clore, G. M. (2016) A simple and robust protocol for high-yield expression of perdeuterated proteins in Escherichia coli grown in shaker flasks. *J. Biomol. NMR* **66**, 85–91
43. Cai, M., Huang, Y., Craigie, R., and Clore, G. M. (2019) A simple protocol for expression of isotope-labeled proteins in Escherichia coli grown in shaker flasks at high cell density. *J. Biomol. NMR* **73**, 743–748
44. Cai, M., Huang, Y., Lloyd, J., Craigie, R., and Clore, G. M. (2021) A simple and cost-effective protocol for high-yield expression of deuterated and selectively isoleucine/leucine/valine methyl protonated proteins in Escherichia coli grown in shaker flasks. *J. Biomol. NMR* **75**, 83–87
45. Sparks, S., Temel, D. B., Rout, M. P., and Cowburn, D. (2018) Deciphering the "fuzzy" interaction of FG nucleoporins and transport factors using small-angle neutron scattering. *Structure* **26**, 477–484.e4
46. Lichtenecker, R. J., Coudevylle, N., Konrat, R., and Schmid, W. (2013) Selective isotope labelling of leucine residues by using alpha-ketoacid precursor compounds. *Chembiochem* **14**, 818–821
47. Paulson, E. K., Morcombe, C. R., Gaponenko, V., Dancheck, B., Byrd, R. A., and Zilm, K. W. (2003) Sensitive high resolution inverse detection NMR spectroscopy of proteins in the solid state. *J. Am. Chem. Soc.* **125**, 15831–15836
48. Neidhardt, F. C., Bloch, P. L., and Smith, D. F. (1974) Culture medium for enterobacteria. *J. Bacteriol.* **119**, 736–747
49. Delaglio, F., Grzesiek, S., Vuister, G. W., Zhu, G., Pfeifer, J., and Bax, A. (1995) NMRPipe: a multidimensional spectral processing system based on UNIX pipes. *J. Biomol. NMR* **6**, 277–293
50. Lee, W., Tonelli, M., and Markley, J. L. (2015) NMRFAM-SPARKY: enhanced software for biomolecular NMR spectroscopy. *Bioinformatics* **31**, 1325–1327